Fuel 90 (2011) 449–458

Contents lists available at ScienceDirect

Fuel

journal homepage: www.elsevier.com/locate/fuel

Effect of spark timing and load on a DISI engine fuelled with 2,5-dimethylfuran

Ritchie Daniel [a], Guohong Tian [a,b], Hongming Xu [a,*], Miroslaw L. Wyszynski [a], Xuesong Wu [a,c], Zuohua Huang [c]

[a] University of Birmingham, Birmingham, B15 2TT, UK
[b] Sir Joseph Swan Centre, Newcastle University, Newcastle Upon Tyne, NE1 7RU, UK
[c] State Key Laboratory of Multiphase Flow in Power Engineering, Xi'an Jiaotong University, Xi'an, China

ARTICLE INFO

Article history:
Received 8 September 2010
Received in revised form 4 October 2010
Accepted 6 October 2010
Available online 20 October 2010

Keywords:
2,5-Dimethylfuran
DMF
Biofuel
Ethanol
SI engines

ABSTRACT

Currently, bioethanol leads the automotive fuel market as the main substitute for gasoline in spark-ignition engines. However, worldwide interest has been triggered in the potential of 2,5-dimethylfuran, known as DMF, since the discovery of improved production methods. Although the energy content of DMF is comparable to that of gasoline, little is known about its combustion characteristics and emissions. Therefore, this work examines the effect of DMF in a single cylinder direct-injection spark-ignition engine. The results are compared to ethanol and gasoline using the optimized spark timings for gasoline and the respective fuel. In summary, DMF produces competitive combustion and emissions qualities to gasoline, which, in some cases surpass ethanol. The two biofuels have a higher burning rate and lower initial combustion duration than gasoline. They also produce greater combustion efficiency, which helps to lower hydrocarbon and carbon monoxide emissions. These initial results highlight how DMF, which was originally only considered as an octane improver, has the potential to become a competitive renewable gasoline alternative.

1. Introduction

In recent years, efforts have been made by the automotive industry to reduce the dependence on fossil fuel supplies and address the increasing public concern of global warming. The outcome from sustained research and development is now commercially evident. In Brazil, flex-fuel vehicles are commonplace; vehicles can sustainably cope with any blend of ethanol and gasoline [1]. This response highlights the potential of biomass-derived fuels to provide a short- to mid-term source of renewable energy, while reducing the impact of CO_2.

Recently, significant breakthroughs have improved the production methods of 2,5-dimethylfuran (DMF) [2]. Dumesic and his team have demonstrated advances in the biomass-to-liquid conversion of fructose into DMF with high efficiency and yield [2,3]. This concept was further developed by Zhao and his co-workers, who observed high yields of 5-hydroxymethylfurfural, or HMF (the intermediate for DMF), without the need for acid catalysts used by Dumesic and his team [4]. Not only does Zhao's method dramatically reduce the production costs, but it now includes glucose as a potential feedstock for HMF. Furthermore, Mascal has reported that cellulose itself can be converted into furanic products [5]. Such advances have attracted attention towards DMF as a potential gasoline alternative [6].

DMF's physicochemical properties are competitive to ethanol. Firstly, its energy density (31.5 MJ/l) is 40% higher than ethanol (23 MJ/l) and much closer to gasoline (35 MJ/l) [7]. Secondly, it has a higher boiling point (92 °C) than ethanol (78 °C), which makes it less volatile and more practical as a liquid fuel for transportation [7]. Thirdly, unlike ethanol, DMF is insoluble in water, which makes it stable in storage and unlikely to contaminate underground supplies or be contaminated by water in transportation pipelines [2]. Finally, DMF offers better anti-knock qualities than gasoline and similar to ethanol, whose research octane number, or RON, is 106 [8]. This will allow the use of high compression ratios or forced induction technology to maximize the thermal efficiency and power [9]. Together with the aforementioned improved production techniques, these physicochemical properties make DMF a very promising gasoline alternative biofuel.

Although researchers have explored many different alcohol based gasoline alternatives [10–12], it is ethanol that has sustained worldwide interest. Current focus hinges on the effect of different ethanol–gasoline blends on a spark-ignition engine [13–16]. Ethanol's high knock tolerance can improve the thermal efficiency and torque output [17]. However, to address the shortcomings of its poor fuel economy caused by the low calorific value, higher compression ratios and boosted technologies are now being used [18].

* Corresponding author.
E-mail address: h.m.xu@bham.ac.uk (H. Xu).

0016-2361/$ - see front matter Crown Copyright © 2010 Published by Elsevier Ltd. All rights reserved.
doi:10.1016/j.fuel.2010.10.008

Definitions, acronyms, abbreviations

aTDC	after top dead centre
bTDC	before top dead centre
CAD	crank angle degrees
CA50	Crank angle at 50% MFB
CO	carbon monoxide
CO_2	carbon dioxide
COV	coefficient of variation
DISI	direct-injection spark-ignition
DMF	2,5-dimethylfuran
ETH	ethanol
HC	hydrocarbon
IMEP	indicated mean effective pressure
ISFCE	gasoline equivalent indicated specific fuel consumption
KL-MBT	knock-limited maximum brake torque
LCV	lower calorific value
MBT	maximum brake torque
MFB	mass fraction burned
NO_X	nitrogen oxides
PM	particulate matter
RON	research octane number
RPM	revolutions per minute
ULG	unleaded gasoline

Currently, few publications can be found on DMF as a gasoline alternative fuel. Studies by Wu et al., which include the laminar burning velocity [19] and the combustion intermediates of DMF [20], were the first to be reported. Recently, the first report on its application as an engine fuel has been made by the authors of this paper. This includes a preliminary experimental comparison of the combustion and emissions performance of DMF, ethanol and gasoline using fixed spark timing regardless of engine load [21]. A second paper by the authors, then compared the laminar burning velocities to both ethanol and gasoline [22].

In this paper, a more extensive investigation into the combustion and emissions effects of advancing the spark timing with load using DMF is reported. The results are compared to ethanol and gasoline using, not only the optimized spark timings for gasoline, but also the respective fuel. Once again, DMF is benchmarked against gasoline and compared to the current leading biofuel, ethanol. It forms part of a series of experiments, led by this institution, to explore the use of DMF as a fuel for automotive applications. The following sections will explain the experimental setup, discuss the results and finally summarize the conclusions.

2. Experimental setup

2.1. Engine and instrumentation

The experiments were performed on a single-cylinder, 4-stroke spark-ignition research engine, as shown in Fig. 1. The 4-valve cylinder head includes the Jaguar spray-guided direct-injection technology used in their V8 production engine (AJ133) [23]. It also includes variable valve timing technology for both intake and exhaust valves. The valve timing used in this study is shown in Table 1.

The engine was coupled to a DC dynamometer to maintain a constant speed of 1500 rpm (±1 rpm) regardless of the engine torque output. The in-cylinder pressure was measured using a Kistler 6041A water-cooled pressure transducer which was fitted to the side-wall of the cylinder head. The signal was then passed to a Kistler 5011 charge amplifier and finally to a National Instruments data acquisition card. Samples were taken at 0.5CAD intervals for 300 consecutive cycles, so that an average could be taken. The crankshaft position was measured using a digital shaft encoder. Coolant and oil temperatures were controlled at 85 °C and 95 °C

Table 1
Engine specification.

Engine type	4-Stroke, 4-valve
Combustion system	Spray guided DISI
Swept volume	565.6 cm^3
Bore × Stroke	90 × 88.9 mm
Compression ratio	11.5:1
Engine speed	1500 rpm
Injector	Multi-hole Nozzle
Fuel pressure and timing	150 bar, 280°bTDC
Intake valve opening	16°bTDC
Exhaust valve closing	36°aTDC

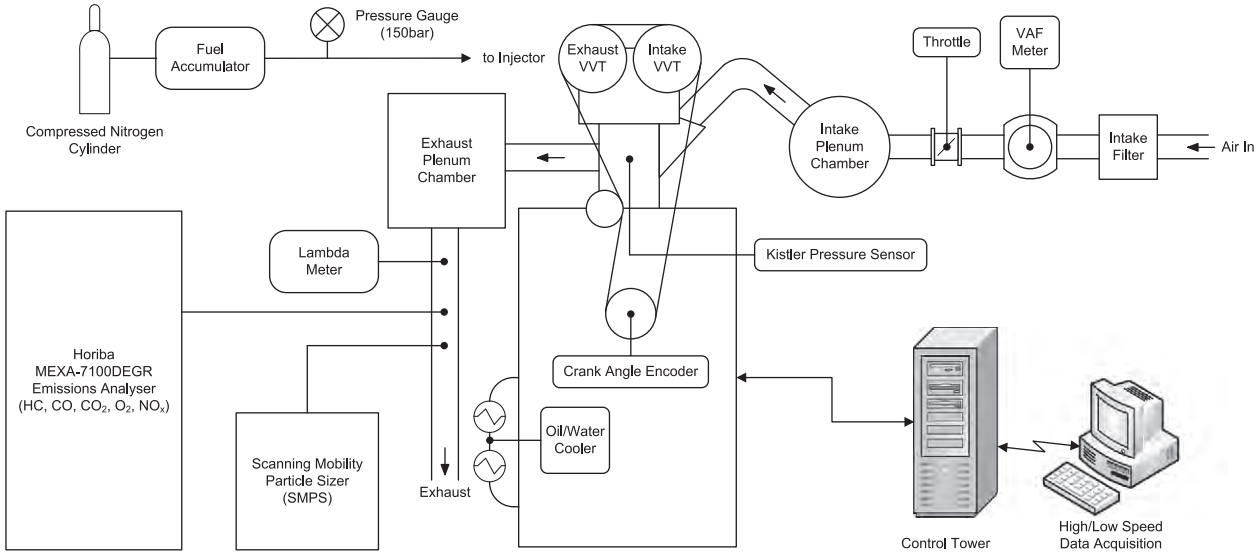

Fig. 1. Schematic of engine and instrumentation setup.

(±3 °C), respectively, using a Proportional Integral Differential (PID) controller. All temperatures were measured with K-type thermocouples.

The engine was controlled using software developed in-house written in the LabVIEW programming environment. High-speed, crank-angle-resolved and low-speed, time-resolved data was also acquired using LabVIEW. This was then analyzed using MATLAB developed code, so that an analysis of the combustion performance could be made.

2.2. Emissions and fuel measurement

The gaseous emissions were quantified using a Horiba MEXA-7100DEGR gas tower. Exhaust samples were taken 0.3 m downstream of the exhaust valve and pumped via a heated line (maintained at 191 °C) to the analyzer.

Particulate matter (PM) emissions were measured using a 3936 Scanning Mobility Particle Sizer Spectrometer (SMPS) manufactured by TSI. This comprises of a 3080 Electrostatic Classifier, a 3775 Condensation Particle Counter (CPC) and a 3081 Differential Mobility Analyzer (DMA). PM samples were taken from the same position as the Horiba analyzer. A heated (150 °C) rotating disc diluter (Model 379020A, supplied by TSI) was used at a dilution ratio of 67:1. The SMPS measured particles from 7.23 to 294.3 nm in diameter and the sample and sheath flow rates were 1 and 10 l/min, respectively.

The fuel consumption was calculated using the volumetric air flow rate (measured by a positive displacement rotary flow meter) and the actual lambda value (Bosch heated LSU wideband lambda sensor and ETAS LA4 lambda meter). The LA4 lambda meter uses fuel-specific curves to interpret the actual air–fuel ratio (AFR) using the oxygen content in the exhaust. Before each test, the user inputs the fuel's hydrogen-to-carbon (H/C) and oxygen-to-carbon (O/C) ratios, as well as the stoichiometric AFR, so that the fuel composition can be used to characterize the fuel curves.

2.3. Test fuels

The DMF used in this study was supplied by Shijiazhuang Lida Chemical Co. Ltd. in China, at 99.8% purity. This was benchmarked against commercial 97 RON gasoline and to bioethanol, both supplied by Shell Global Solutions UK. A high octane gasoline was chosen, as this represents the most favorable characteristics offered by the market, and provides a strong benchmark to the two biofuels. The fuel characteristics are shown in Table 2.

2.4. Experimental procedure

The engine was considered warm once the coolant and lubricating temperatures had stabilized at 85 °C and 95 °C, respectively. All the tests were carried out at the stoichiometric AFR ($\lambda = 1$), fixed injection timing (280°bTDC), ambient air intake conditions (approximately 25 ± 2 °C) and constant valve timing (see Table 1). The pressure data from 300 consecutive cycles was recorded for each test using the in-house developed LabVIEW code.

When changing fuels, the high pressure fuelling system was purged using nitrogen until the lines were considered clean. Once the line was re-pressurized to 150 bar using the new fuel, the engine was run for several minutes. This made sure that no previous fuel remained on the injector tip or any combustion chamber crevices before any data was acquired. The ETAS LA4 lambda meter settings were changed for each fuel using the stoichiometric AFR, O/C and H/C ratios in Table 2.

Table 2
Test fuel properties.

	DMF	Ethanol	Gasoline
Chemical formula	C_6H_8O	C_2H_6O	C_2–C_{14}
H/C ratio	1.333	3	1.795
O/C ratio	0.167	0.5	0
Gravimetric oxygen content (%)	16.67	34.78	0
Density @ 20 °C (kg/m3)	889.7*	790.9*	744.6
Research Octane Number (RON)	n/a	106	96.8
Stoichiometric air–fuel ratio	10.72	8.95	14.46
LHV (MJ/kg)	33.7*	26.9*	42.9
LHV (MJ/L)	30*	21.3*	31.9
Heat of vaporization (kJ/kg)	332	840	373
Initial boiling point (°C)	92	78.4	32.8

* Measured at the University of Birmingham.

2.5. Spark advance

The optimum ignition timing, otherwise known as the MBT timing, was determined for each fuel from spark sweeps generated between 3.5–8.5 bar IMEP in 1 bar IMEP intervals. In this study, it is defined as the ignition timing which gives the maximum IMEP for a fixed throttle position. At each load, the spark timing was advanced to find the knock limit or until a significant drop in performance or stability was seen (torque decrease >5% or COV of IMEP >3%). If audible knock occurred, the MBT timing was retarded by 2CAD. When this occurs, the optimum ignition timing is then referred to as the knock-limited MBT or, KL-MBT timing. Retarding the timing further for emissions preservation was not used, in order to eliminate subjectivity. Similarly, the spark timing was retarded until a similar drop in performance was found. While performing each spark sweep, the fuel and air flow rates were kept constant once the required load and stoichiometric AFR was achieved at the estimated MBT point. Firstly, the throttle position was adjusted and then the fuel injection pulse width was adjusted finely (±1 μs) to find stoichiometry. Three repeats were made with each fuel to produce an average.

2.6. Engine load

Once the MBT timings were determined for each fuel, the engine load was varied once more from 3.5 to 8.5 bar IMEP, in 1 bar IMEP intervals. At each load the engine was run at the MBT/KL-MBT timing for each fuel. When using DMF and ethanol, fixed gasoline MBT/KL-MBT timing was also used to assess the performance under the same ignition conditions. For repeatability, three sets of tests were carried out using each fuel over three consecutive days. However, the test order was varied each day in order to minimize the effect of engine drift.

3. Results and discussion

3.1. Spark advance

The MBT/KL-MBT timings for each fuel are shown in Fig. 2. At low load (3.5 bar IMEP), there is no appreciable difference in the MBT location between the three fuels; the spark sweeps generate a relatively flat IMEP curve around 34°bTDC. However, throughout the remaining load range, ethanol allowed the most advanced spark timing due to its higher anti-knock quality and burning velocity. Ethanol also generates greater charge-cooling because of the higher latent heat of vaporization (see Table 2), which lowers the combustion temperature and discourages end-gas pre-ignition (see Section 3.4). At the highest load, ethanol is 11°bTDC more advanced than gasoline and 5°bTDC more than DMF. Although DMF is limited by audible knock which inhibits the use of MBT timing until 6.5 bar IMEP, the maximum separation between DMF and

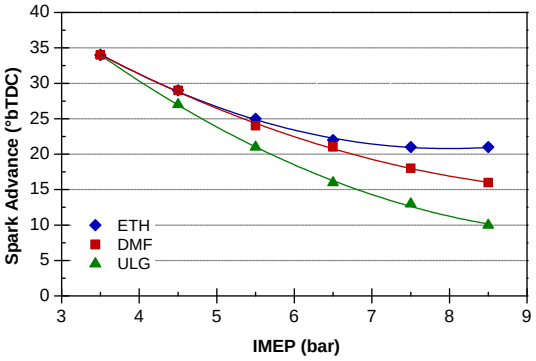

Fig. 2. MBT/KL-MBT spark timings at various engine loads for DMF, ethanol and gasoline.

ethanol is only 1CAD. However, the optimum spark timing for gasoline is clearly the most retarded, once again limited by knock.

When using 97 RON gasoline, a knock margin (2CAD retard) was enforced as early as 4.5 bar IMEP. However, for DMF, this was not enforced until 5.5 bar IMEP. Although this gives DMF a slight advantage over 97 RON gasoline, in terms of knock suppression and therefore spark advance, the anti-knock qualities of DMF are not as proficient as ethanol's. Gautam and Martin have shown that the knock suppression capability of oxygen containing fuels is related to the relative oxygen content [10]. This could explain why knock occurs at lower loads, when using DMF. To overcome the obstacles of knock and increase engine performance, future engine tests by the authors will examine the benefits of two-stage injection strategies as adopted by other researchers [24,25].

3.2. Engine load

In this section, the performance and emissions of DMF are compared to gasoline and ethanol using gasoline MBT/KL-MBT timing and the fuel-specific MBT/KL-MBT timings at the various engine loads. The fuel-specific MBT/KL-MBT results are indicated by solid lines, whereas the gasoline MBT/KL-MBT timing results are shown using broken lines (unless stated otherwise).

3.3. Fuel consumption and combustion efficiency

The effect of gasoline's superior energy density (see Table 2) is clearly seen in Fig. 3 where, relative to gasoline, both DMF and ethanol require more fuel to maintain the required power output. Fig. 3(a) shows the gravimetric indicated specific fuel consumption (ISFC). Here, small gains were found above 5.5 bar IMEP when optimizing the ignition timings. However, gasoline offers much lower fuel mass consumption across the entire load range. Nevertheless, compared to ethanol, DMF consumes less fuel, largely explained by the difference in gravimetric calorific value; DMF is 25% or 6.8 MJ/

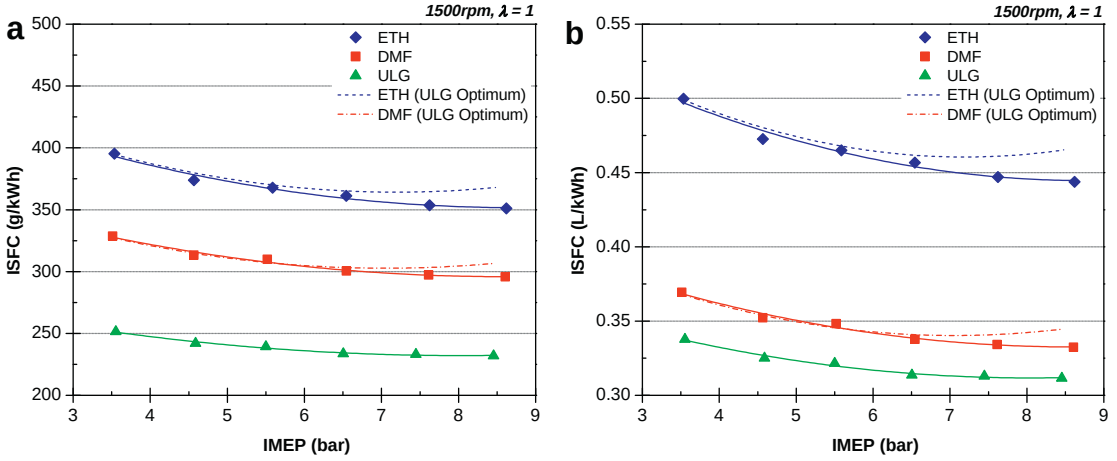

Fig. 3. (a) Gravimetric and (b) volumetric indicated specific fuel consumption.

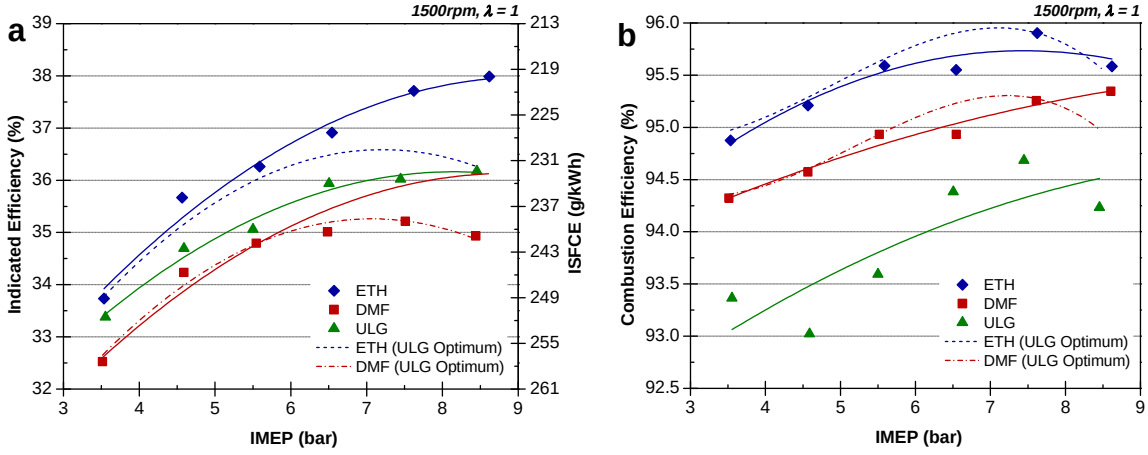

Fig. 4. (a) Indicated efficiency/gasoline equivalent ISFC and (b) combustion efficiency.

kg higher than ethanol (see Table 2). However, the volumetric fuel consumption is normally the benchmark for fuel economy and is shown in Fig. 3(b). Here, the performance of both biofuels is improved relative to gasoline. However, the fuel consumption using DMF is much more similar to that of gasoline, due to a higher density than ethanol and a similar volumetric calorific value to gasoline.

Another method of interpreting the fuel conversion efficiency is through the gasoline equivalent fuel consumption, or ISFCE, using Eq. (1). This eliminates the effect of the calorific value on the fuel consumption and provides an insight into the efficiency of combustion.

$$\text{Gasoline Equivalent Fuel Consumption}: \ \text{ISFCE}_x = \frac{\text{ISFC}_x \times \text{LHV}_x}{\text{LHV}_{ULG}} \quad (1)$$

Similarly, the indicated engine thermal efficiency can be used to assess the relative fuel performance. The combined results of ISFCE and the indicated engine thermal efficiency are shown in Fig. 4(a). Under gasoline MBT/KL-MBT timing, the three fuels peak between 7–7.5 bar IMEP. Previous modeling investigations have shown how the temperature of DMF combustion is the highest [21], which could help to explain why the indicated efficiency is the lowest (see also Section 3.4). Higher combustion temperatures generate greater heat loss through the cylinder walls reducing the conversion of fuel energy into useful work. The greater heat rise is mainly due to DMF's lower heat of vaporization (Table 2); despite requiring relatively less energy to break the intermolecular bonds, more energy is lost through higher combustion temperatures. The result is low indicated efficiency. This is also reflected in the ISFCE. When using fuel-specific MBT/KL-MBT timing, however, DMF becomes competitively efficient to gasoline over 8 bar IMEP. Furthermore, the limitations of the higher stoichiometric AFR of gasoline (see Table 2) suggest that higher efficiencies can be found using the biofuels at even higher loads (and throttle positions) than were tested, based on the current trend. This could theoretically increase the efficiency of DMF beyond that of gasoline.

The indicated efficiency, however, does not explain the completeness of combustion. This requires an analysis of the incomplete combustion products (e.g. unburned hydrocarbons (HC) and carbon monoxide (CO) emissions), which represent the combustion inefficiency. During the combustion process, not all the chemical energy is released. The fraction that is burned, compared to that which is supplied, is expressed by the combustion efficiency [26]. This is calculated using Equation 2 [27]:

$$\text{Combustion Efficiency}: \ \eta_c = 1 - \frac{\sum x_i Q_{\text{LHV}_i}}{[\dot{m}_{\text{fuel}}/(\dot{m}_{\text{air}} + \dot{m}_{\text{fuel}})]Q_{\text{LHV}_{\text{fuel}}}} \quad (2)$$

where x_i and Q_{LHVi} represent the mass fractions and lower heating values (LHV) of HC, CO, nitric oxide (NO) and hydrogen (H_2), respectively. For this work, Q_{LHVHC} has been treated equal to $Q_{LHVfuel}$. In reality, the HC emissions contain different components or species, which have different enthalpies of formation or LHV. In future work, the authors intend to quantify these species in order to better understand the combustion efficiency of each fuel.

According to Heywood, the typical range of combustion efficiency, for spark-ignition engines operating under lean conditions, is between 95–98% [26]. The results for this investigation are shown in Fig. 4(b). Between the three fuels, ethanol consistently offers the highest combustion efficiency, closely followed by DMF and then gasoline. This is largely due to the relative oxygen content. Although, paradoxically, the oxygen hinders the fuel consumption performance because it offers no additional energy, it does help to improve the completeness of combustion. Using gasoline MBT/KL-MBT timing, the peak combustion efficiency coincides with the peak indicated efficiency (Fig. 4(a)), which similarly decays after 7–7.5 bar IMEP. The cross-over using DMF and ethanol around 8 bar IMEP is caused by the over-retarded combustion for knock avoidance using gasoline MBT/KL-MBT timing, which reduces the available combustion time.

3.4. In-cylinder pressure and temperature

The maximum in-cylinder pressure or P_{max} is shown for the three fuels in Fig. 5(a). For gasoline MBT/KL-MBT timing, there are clear differences between the fuels at all loads. At low loads, ethanol produces the highest combustion pressure; at 3.5 bar IMEP, the P_{max} using ethanol is 1 bar higher than for both DMF and gasoline. However, at high load, the P_{max} using DMF exceeds ethanol and gasoline by a similar amount. This effect is similar to that seen with the initial combustion duration shown in Fig. 7. At low loads, the ethanol–air mixture reacts quicker than with DMF. However, at high loads, this trend is reversed and the lower initial combustion duration for DMF results in a higher P_{max}. This might also be due to higher fuel burning temperatures compared to ethanol and gasoline. When using fuel-specific ignition timing, the P_{max} for ethanol exceeds DMF due to the more advanced ignition timing.

The theoretical maximum in-cylinder gas temperatures or T_{max} are shown in Fig. 5(b). This is calculated using a detailed engine gas-dynamics and thermodynamics model, which was used in a previous publication [21]. Here, the experimental and simulated IMEPs and P_{max} agree to within 99.67%. The higher latent heat of vaporization of ethanol (see Table 2) encourages a greater charge-cooling effect than with gasoline and DMF, which reduces the T_{max} and P_{max} for the same ignition timing. More thermal energy is absorbed to evaporate the liquid ethanol in the combustion chamber, whereas less energy is required for gasoline and DMF to change phase, producing more net heat. Previous tests by the authors highlighted the similarity in T_{max} between gasoline and DMF [21]. However, when using fuel-specific MBT/KL-MBT timing, the T_{max} when using DMF is much higher than with gasoline, due to the slightly lower latent heat of vaporization of DMF. At 8.5 bar IMEP, the T_{max} when using DMF is 120 °C greater than with gasoline, significantly impacting the NO_x emissions (see Fig. 10(a)). The increase in T_{max}, when using optimized ignition timing, is also seen with ethanol. For example, at approximately 8.5 bar IMEP, the T_{max} when using ethanol is only 17 °C lower than with gasoline. This is a significant increase compared to the difference of 286 °C, when using gasoline MBT/KL-MBT timing, which again significantly effects the NO_x emissions (see Section 3.7).

3.5. Volumetric efficiency and pumping loss

The comparison of the pumping losses between DMF and ethanol highlight the influence of the different physicochemical properties and their effect on fuel economy. By weight, ethanol contains more oxygen molecules, which results in a lower stoichiometric AFR (Table 2). This reduces the throttle angle demand and as a result increases the net pumping losses and fuel consumption. On initial inspection, this behavior explains the trend of the volumetric efficiency compared to DMF and gasoline (Fig. 6). Although at lower loads (<6 bar IMEP), there is little difference between the oxygen content fuels, at higher loads ($\geqslant$6 bar IMEP), the separation is more evident, which demonstrates the effect of ethanol's lower stoichiometric AFR. For gasoline, whose stoichiometric AFR is much higher (Table 2), the volumetric efficiency is superior because more air is required to compensate for no oxygen in the fuel. However, with closer inspection of the pumping losses below 6 bar IMEP, ethanol overcomes the higher throttling requirement. This is largely due to the higher charge-cooling effect of ethanol. At

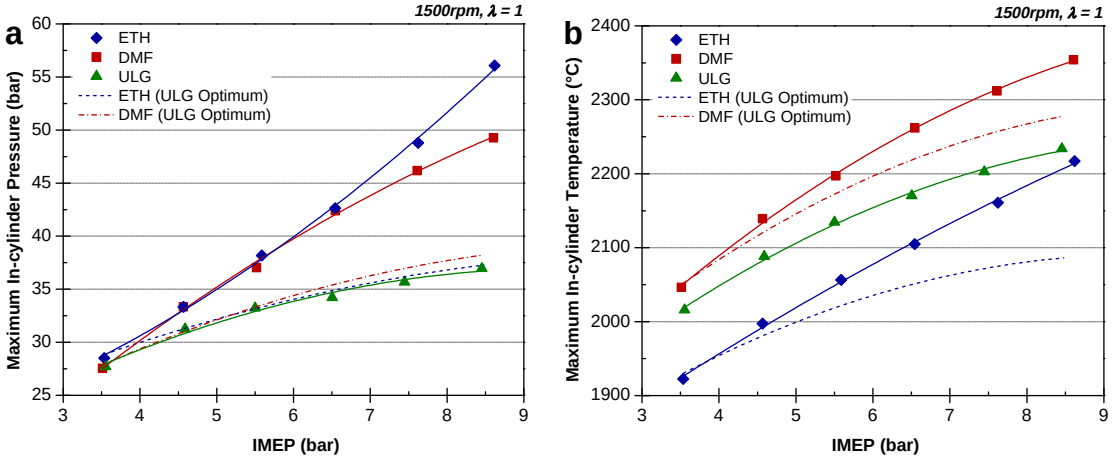

Fig. 5. (a) Maximum in-cylinder pressures and (b) simulated temperatures.

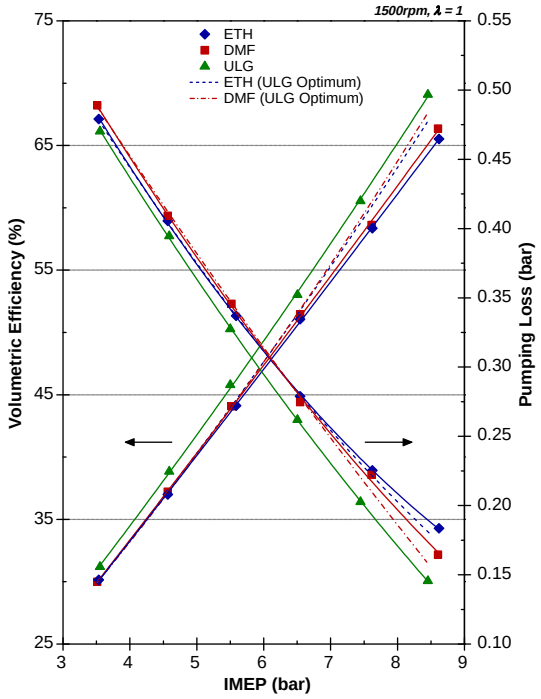

Fig. 6. Volumetric efficiency and pumping losses.

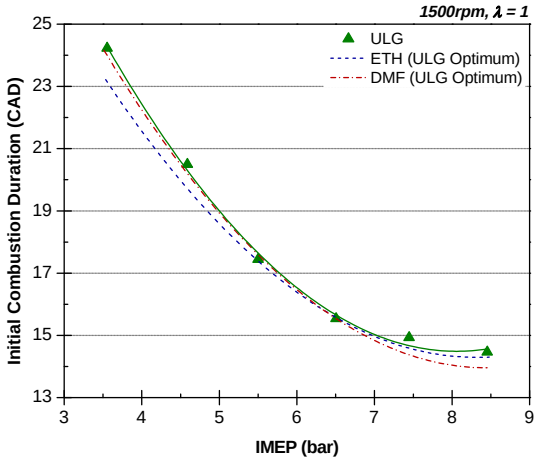

Fig. 7. Initial combustion durations (gasoline MBT/KL-MBT).

8.5 bar IMEP, the pumping loss, when fuelled with DMF at gasoline MBT/KL-MBT timing is 157 kPa, whereas for ethanol this is 178 kPa, an advantage to DMF of 21 kPa. However, at 3.5 bar IMEP, this advantage shifts to ethanol by 10 kPa, highlighting the impact of its higher heat of vaporization. This effect on volumetric efficiency in a direct-injection spark-ignition engine is well documented [26,28–30] and helps to counteract the pumping losses due to throttling. However, at loads above 6 bar IMEP, the charge-cooling advantage is superseded by the relative throttling losses incurred.

3.6. Combustion phasing

Fig. 7 shows the variation in initial combustion duration between the three fuels, defined as the crank angle degrees (CAD) between the spark timing and the 5% mass fraction burned (MFB). The MFB is calculated from the heat release analysis using the standard method as described by Stone [30]. The fuel-specific MBT/KL-MBT data has been removed so that a comparison can be made under the same spark timings. This variation in initial combustion duration can help to explain the maximum in-cylinder pressures; lower durations result in higher combustion pressures as the pressure rise occurs earlier in the combustion stroke. The faster burning rate of ethanol compared to gasoline has been reported by several researchers [10,31–33]. At 3.5 bar IMEP, the initial combustion duration using ethanol was 0.9CAD lower than DMF, which can be explained by the higher laminar flame speed [22]. However, at 8.5 bar IMEP, the initial combustion duration using DMF is now 0.3CAD lower than ethanol. This is due to higher in-cylinder temperatures when using DMF (Fig. 5(b)), which increases the burning speed [22].

This faster burning rate of the biofuels compared to gasoline is shown by the combustion duration in Fig. 8, defined as the as 10–90% MFB period in CAD. At fixed gasoline MBT/KL-MBT timing, DMF burns the fastest (apart from 3.5 bar IMEP). At 8.5 bar IMEP, DMF burns 1CAD faster than ethanol and 1.3CAD faster than gasoline. Using fuel-specific MBT/KL-MBT timings, the combustion durations reduce further. At 8.5 bar IMEP, the combustion duration of the biofuels is 4CAD less than gasoline. Once again, apart from the extreme high and low loads (3.5 bar and 8.5 bar IMEP), the combustion duration is marginally lower (at least 0.35CAD) when using DMF, than for ethanol.

Fig. 9 shows the combustion durations either side of the 50% MFB point, or CA50, using gasoline MBT/KL-MBT timing at

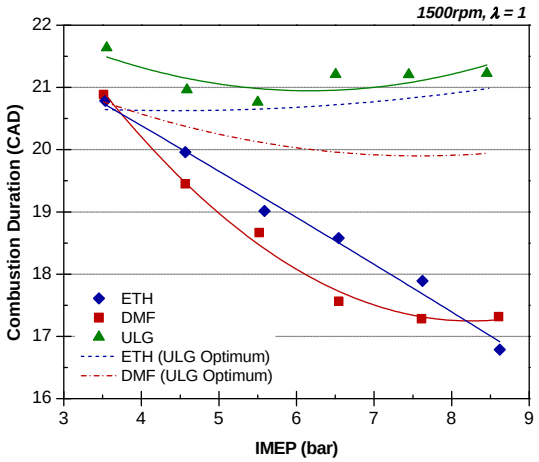

Fig. 8. Combustion durations (10–90% MFB).

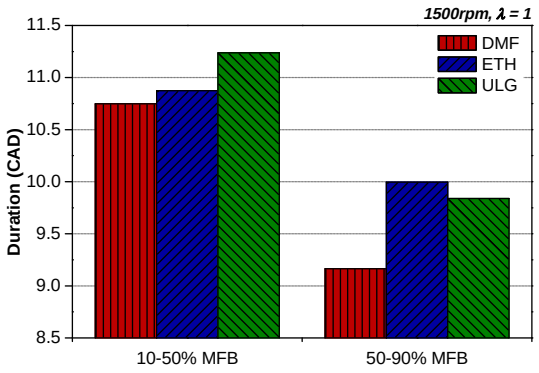

Fig. 9. Combustion durations either side of CA50 (8.5 bar IMEP, gasoline KL-MBT timing).

8.5 bar IMEP. For all three fuels, the duration before CA50 (10–50% MFB), is slightly higher than afterwards (50–90% MFB). For DMF, the combustion is consistently quicker than ethanol; the 10–50% MFB duration is 0.12CAD lower than ethanol and the 50–90% MFB duration is 0.83CAD lower. The reduction in duration after the CA50 location using DMF is also 3% and 7% higher than for gasoline and ethanol, respectively, highlighting the high burning speed when using DMF.

These results highlight the advantage of the burning speed of DMF combustion compared to that when using ethanol, despite DMF combustion having a lower measured laminar flame speed [22]. Overall, however, under these test conditions, both oxygen content fuels burn more quickly in the 10–90% MFB range than gasoline.

3.7. Standard emissions

The engine-out emissions are compared between the three fuels at the various loads and spark timings. Firstly, the traditional legislated emissions are evaluated, including the HC, CO and nitrous oxide (NO_x) emissions, followed by an analysis of the carbon dioxide (CO_2) emissions.

The formation of NO_x increases very strongly with combustion temperature [30]. Fig. 10(a) shows the production of indicated specific NO_x ($isNO_x$) for all the test conditions. It is clear that the $isNO_x$ production generally increases with load. When using gasoline MBT/KL-MBT timing, ethanol produces much lower $isNO_x$ emissions compared to gasoline. This is because ethanol burns at a relatively higher rate (Fig. 8) and lower temperature (Fig. 5(b)). Although DMF appears to have a marginally quicker burning rate than ethanol, the $isNO_x$ emissions are more similar to gasoline because the combustion temperatures are much higher (Fig. 5(b)). For fuel-specific ignition timing, the production of $isNO_x$ emissions increases. For ethanol, this increase with load is much larger than for DMF and above 7.5 bar IMEP, the emissions are now comparable to gasoline. Optimized ignition timing for ethanol is 11CAD more advanced than the gasoline MBT/KL-MBT timing, which rapidly increases the in-cylinder pressures (Fig. 5(a)). The peak combustion pressures for DMF are similar to ethanol but the temperatures are somewhat higher due to the lower charge-cooling effect. The relative $isNO_x$ emissions can also be attributed to the H/C ratio. Ethanol, which produces the lowest $isNO_x$ emissions, has the highest H/C ratio, whereas DMF produces the highest $isNO_x$ emissions and has the lowest H/C ratio (see Table 2). Therefore, the $isNO_x$ emissions have an inverse relationship to the H/C ratio, a trend first reported in the publication by Harrington and Shishu [34].

As shown in Fig. 10(b), the indicated specific total hydrocarbon emissions (isTHC) for DMF are competitive to gasoline. However, more significantly, the isTHC emissions are much lower for ethanol. Ethanol's much higher oxygen content compared to DMF (Table 2), together with its higher combustion efficiency (Fig. 4(b)), aids the oxidation of unburned hydrocarbons, as oxygen is more readily available. As the load increases from 3.5–8.5 bar IMEP, the isTHC emissions decrease by approximately 30% for all fuels. This is due to increased combustion temperatures (Fig. 5(b)) and thus combustion efficiencies (Fig. 4(b)) because of greater oxidation of the hydrogen and carbon molecules. However, the reduced sensitivity of the FID analyzer to oxygen content fuels suggests that the total hydrocarbon emissions for ethanol and DMF are higher [35,36]. This necessitates a detailed hydrocarbon emissions investigation for accurate quantification.

The indicated specific carbon monoxide emissions (isCO) comparison between is made in Fig. 10(c). Similarly to the isTHC emissions (Fig. 10(b)), the isCO emissions generally decrease as load increases. The trend is similar to the ISFCE (Fig. 4(a)), where the lowest isCO emissions arise at the highest efficiency. Between the two oxygen content fuels, ethanol consistently produces the lowest isCO emissions. This is due to a higher combustion efficiency and oxygen content. Under gasoline MBT/KL-MBT timing, the difference increases with load. At 3.5 bar IMEP, ethanol is 1 g/kWh lower, whereas at 8.5 bar IMEP, this difference increases to 3 g/kWh. Under fuel-specific ignition timing, the largest difference is seen at medium loads. For gasoline, the relationship with load is less predictable. The peak at 4.5 bar IMEP could be explained by the relatively lower combustion efficiency at this point (Fig. 4(b)). At this load, the mixture may be inhomogeneous, resulting in localized pockets of fuel-rich mixture and more incomplete combustion. However, the remaining isCO emissions fluctuate within a similar range as the two biofuels, which all decrease to a minimum between 7–7.5 bar IMEP.

Although carbon dioxide (CO_2) is a non-toxic gas, which is not classified as a pollutant engine emission, it is one of the substances responsible for global temperature rises through the greenhouse effect. Therefore, a consideration of the indicated specific CO_2 ($isCO_2$) production is made between the three fuels (Fig. 10(d)). The $isCO_2$ emissions decrease with increasing load and advancing ignition timing towards the MBT/KL-MBT timing. The $isCO_2$ emissions are an indication of the completeness of combustion. Therefore, as the load is increased, the combustion is more complete, which is shown by the increase in combustion efficiency in Fig. 4(b). When using gasoline MBT/KL-MBT timing, DMF and ethanol combustion produces a peak in efficiency between 6–7 bar IMEP and a minimum in $isCO_2$. Although both biofuels produce

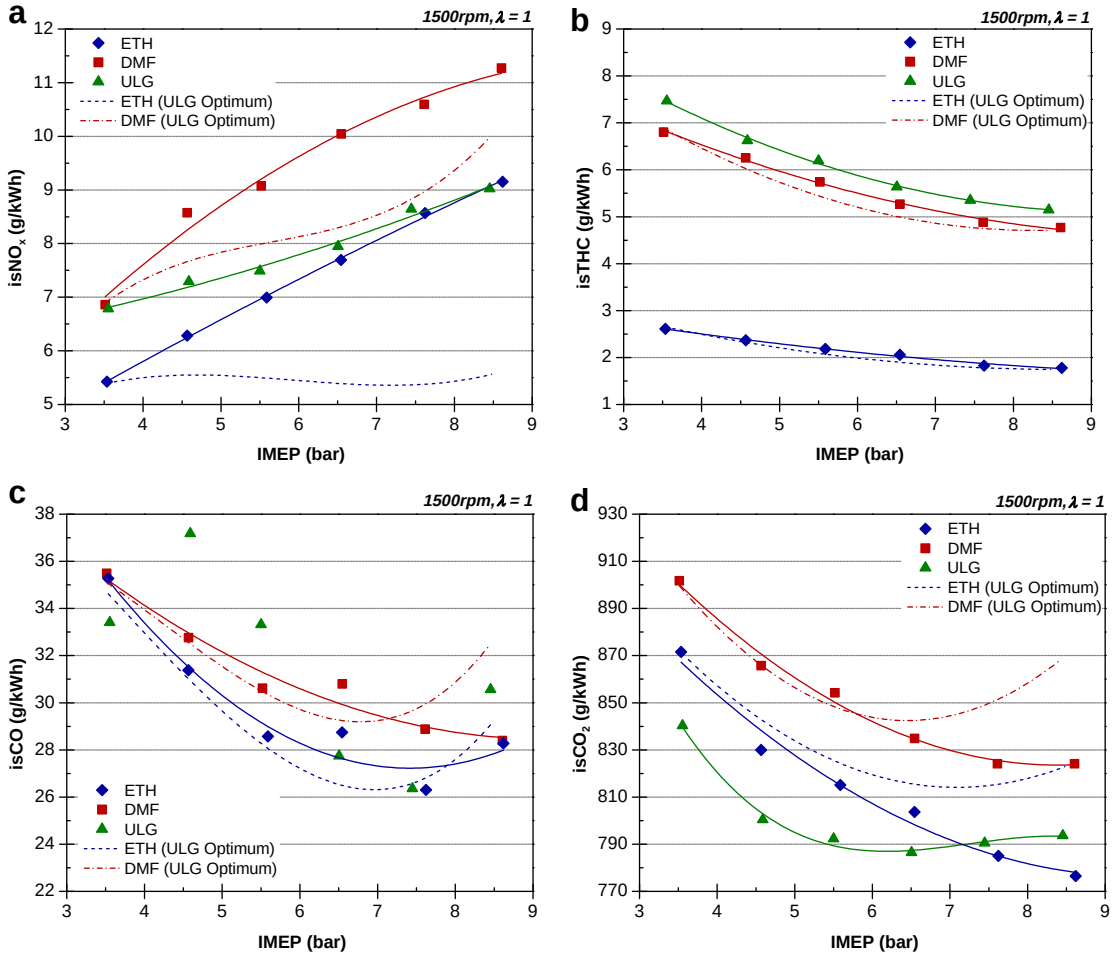

Fig. 10. Indicated specific emissions (a) NOx, (b) THC, (c) CO and (d) CO_2.

higher engine-out isCO_2 emissions than gasoline, they both have the added benefit of consuming the CO_2 in the atmosphere during their raw production. Therefore, it is fairer to compare the relative lifecycle CO_2 emissions. This, however, is outside the scope of this work.

3.8. PM emissions

The PM size distributions for the three fuels at 3.5 bar IMEP using gasoline MBT timing (34°bTDC), are shown in Fig. 11(a). Typically, the PM size distribution consists of two modes: the accumulation and nucleation modes. The former consists of solid carbonaceous species usually greater than 50 nm in diameter, whereas the latter consists of liquid particles usually less than 50 nm in diameter [37]. The separation between the nucleation and accumulation modes is shown clearly by the peak in the size distributions around 50 nm in Fig. 11(a). At this low load, the size distribution shows marginally more accumulation mode particles than nucleation ones. For gasoline, 62.1% of the total particles are accumulation mode particles, whereas for DMF and ethanol, this rises to 64.4% and 67.1%, respectively. The difference between DMF and ethanol is 21,805 particles/cm^3. This might be caused by DMF's lower viscosity and surface tension, which leads to smaller injected fuel particles [38]. Also, the in-cylinder temperature when using ethanol (Fig. 5(b)) is much lower than for DMF. This is caused by the greater charge-cooling effect when using ethanol, which counteracts the benefit that the higher oxygen content (Table 2) would have in helping to lower the PM emissions.

The PM size distributions are also compared at 8.5 bar IMEP using gasoline KL-MBT timing (10°bTDC). This is shown in Fig. 11(b). Evidently, the effect of load has a significant impact on the PM emissions. The separation between the nucleation and accumulation modes is shown clearly by the inflection in the size distributions around 50 nm in Fig. 11(b). Here, the nucleation mode particles dominate the particle size distribution for each fuel, with peaks between 25–30 nm. For ethanol and DMF, the accumulation mode now only represents 2.1% and 1.7%, of the total particle concentrations, respectively. However, for gasoline, the proportion of accumulation mode particles is much higher (18.3%). In absolute terms, gasoline combustion also produces more accumulation mode particles than when fuelled with the biofuels; both biofuels produce less than 4000 particles/cm^3, whereas gasoline produces almost 21,000 particles/cm^3. This is likely to be caused by the higher droplet velocity of gasoline and relatively high mean droplet diameter, found in previous studies [38]. This could increase the impingement on the piston surface, which would explain why the relatively lower combustion efficiency is seen in Fig. 4(b). At this load, the biofuels also burn at higher pressures and temperatures (Fig. 5), which helps to promote pyrolysis and further reduce the solid carbonaceous emissions. The opposite is true, however, for gasoline when considering the nucleation mode concentration at 8.5 bar IMEP. Now, gasoline combustion produces a similar amount of particles to that of ethanol, and DMF is the worst offender; almost 122,000 particles/cm^3, or 30% more particles are produced when using DMF. This relative increase in nucleation mode particles for DMF was seen in previous experiments by the

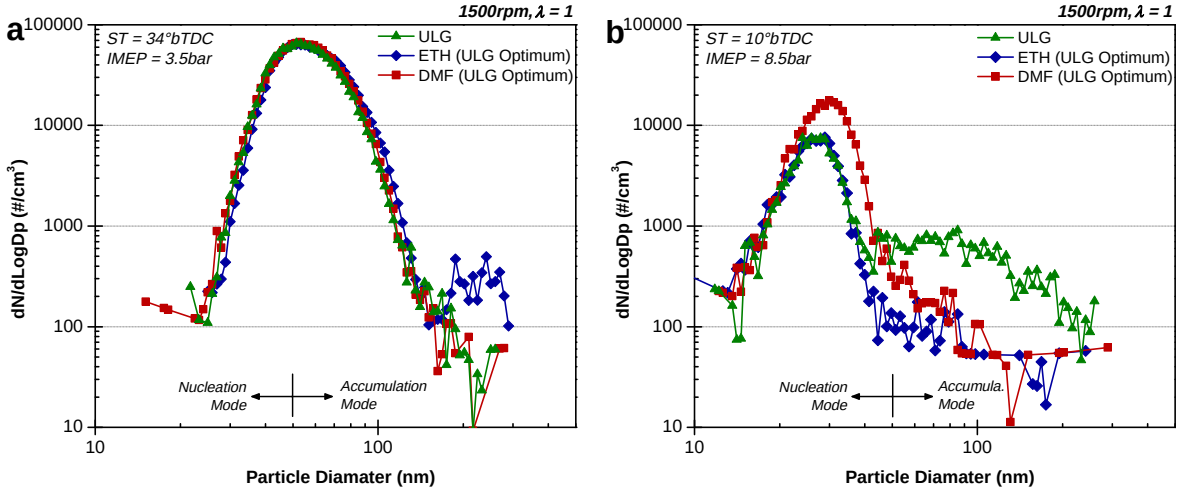

Fig. 11. (a) PM size distributions at 3.5 bar and (b) 8.5 bar IMEP using gasoline MBT/KL-MBT timing.

authors [21] and is likely to be caused by the incomplete combustion of the ring structure of DMF, which are known to be soot precursors [39,40]. Further investigations into the PM emissions using DMF and the impact of the volatile components are underway.

4. Conclusions

This study compares the performance and emissions of a novel biofuel, known as DMF (2,5-dimethylfuran), with commercial gasoline and bioethanol. All tests were performed on a single cylinder spark-ignition direct-injection engine at various engine loads from 3.5–8.5 bar IMEP in 1 bar intervals. The engine was tested using each fuel at the optimized gasoline ignition timing and at the fuel-specific optimized timings. Based on these experiments, the following conclusions can be drawn:

1. Unlike gasoline and DMF, ethanol combustion was not limited by knock, which allowed the MBT timing to be used. Despite this, DMF was more resistant to knock than gasoline.
2. When using gasoline MBT/KL-MBT timings, DMF combustion was faster than with ethanol. DMF and ethanol have lower initial and total combustion durations than gasoline especially with advanced ignition timing, highlighting the rapid combustion of these oxygen content fuels.
3. The volumetric fuel consumption rate of DMF is similar to that of gasoline; a consumer using DMF as a substitute for gasoline, could benefit from a similar driving range.
4. DMF combustion efficiency is higher than for gasoline, but the indicated efficiency is lower: more thermal energy is lost when using DMF, due to higher combustion temperatures.
5. With the exception of NO_x, the engine-out emissions of DMF are similar, if not lower, than with gasoline.
6. When using gasoline MBT/KL-MBT timing, the PM emissions for DMF are comparable to gasoline at low load (3.5 bar IMEP). At high load (8.5 bar IMEP), DMF produces higher nucleation mode particles than gasoline but lower accumulation mode particles.

Overall, these experiments highlight the competition DMF creates with ethanol in replacing gasoline as a spark-ignition fuel. Future engine investigations are planned to supplement these findings and further examine the case for DMF. This includes the use of different fuel blends, various modeling and optical engine studies, as well as a full investigation into the unregulated and toxic emissions.

Acknowledgments

The present work is part of a 3-year research project sponsored by the Engineering and Physical Sciences Research Council (EPSRC) under the grant EP/F061692/1. The authors would like to acknowledge the support from Jaguar Cars Ltd., Shell Global Solutions and various research assistants and technicians. Finally, the authors would like to acknowledge the support from their international collaborators at Tsinghua University, China.

References

[1] Bastian-Pinto C, Brandão L, Lemos Alves M. Valuing the switching flexibility of the ethanol–gas flex fuel car. Annu Oper Res 2010;176:16.
[2] Roman-Leshkov R, Barrett CJ, Liu ZY, Dumesic JA. Production of dimethylfuran for liquid fuels from biomass-derived carbohydrates. Nature 2007;447:982–6.
[3] Dumesic JA, Roman-Leshkov Y, Chheda JN. Catalytic process for producing furan derivatives from carbohydrates in a biphasic reactor. US: World Intellectual Property; 2007.
[4] Zhao H, Holladay JE, Brown H, Zhang ZC. Metal chlorides in ionic liquid solvents convert sugars to 5-hydroxymethylfurfural. Science 2007;316:1597–600.
[5] Mascal M, Nikitin EB. Direct, high-yield conversion of cellulose into biofuel. Angewandte Chemie Int Ed 2008;47:7924–6.
[6] Luque R, Herrero-Davila L, Campelo JM, Clark JH, Hidalgo JM, Luna D, et al. Biofuels: a technological perspective. Energy Environ Sci 2008;1(5):513–93.
[7] Binder JB, Raines RT. Simple chemical transformation of lignocellulosic biomass into furans for fuels and chemicals. J Am Chem Soc 2009;131(5):1979–85.
[8] Mousdale DM. Bio-ethanol as a fuel: biotechnology, biochemical engineering and sustainable development. Boca Raton: CRC Press; 2008.
[9] Nakata K, Uchida D, Ota A, Utsumi S, Kawatake K. The impact of RON on SI engine thermal efficiency. SAE 2007-01-2007; 2007.
[10] Gautam M, Martin DW. Combustion characteristics of higher-alcohol/gasoline blends. IMechE 2000;214 (Part 4).
[11] Zhang F, Shuai S, Wang J, Wang Z. Influence of Methanol Gasoline Blend Fuel on Engine and Catalyst Performance. SAE 2009-01-1182; 2009.
[12] Pourkhesalian AM, Shamekhi AH, Salimi F. Performance and emission comparison and investigation of alternative fuels in SI engines. SAE 2009-01-0936; 2009.
[13] Cooney CP, Yeliana, Worm JJ, Naber JD. Combustion characterization in an internal combustion engine with ethanol–gasoline blended fuels varying compression ratios and ignition timing. Energy Fuels 2009; 23.
[14] Kar K, Cheng W. Effects of ethanol content on gasohol PFI engine wide-open-throttle operation. SAE 2009-01-1907; 2009.
[15] Koc M, Sekmen Y, Topgul T, Yucesu HS. The effects of ethanol–unleaded gasoline blends on engine performance and exhaust emissions in a spark-ignition engine. Renew Energy 2009;34:2101–6.
[16] Kumar A, Khatri DS, Babu MKG. An investigation of potential and challenges with higher ethanol–gasoline blend on a single cylinder spark ignition research engine. SAE 2009-01-0137; 2009.
[17] Nakama K, Kusaka J, Daisho Y. Effect of ethanol on knock in spark ignition gasoline engines. SAE 2008-32-0020; 2008.

[18] Yoon SH, Ha SH, Roh HG, Lee CS. Effect of bioethanol as an alternative fuel on the emissions reduction characteristics and combustion stability in a spark ignition engine. IMechE 2009;223.
[19] Wu X, Huang Z, Jin C, Wang X, Zheng B, Zhang Y, et al. Measurements of Laminar burning velocities and Markstein lengths of 2,5-dimethylfuran–air-diluent premixed flames. Energy Fuels 2009;23:4355–62.
[20] Wu X, Huang Z, Yuan T, Zhang K, Wei L. Identification of combustion intermediates in a low-pressure premixed laminar 2,5-dimethylfuran/oxygen/argon flame with tunable synchrotron photoionization. Combust Flame 2009;156:1365–76.
[21] Zhong S, Daniel R, Xu H, Zhang J, Turner D, Wyszynski ML, et al. Combustion and emissions of 2,5-dimethylfuran in a direct-injection spark-ignition engine. Energy Fuels 2010;24(5):2891–9.
[22] Tian G, Xu H, Daniel R, Li H, Shuai S, Richards P. Laminar burning velocities of 2,5-dimethylfuran compared with ethanol and gasoline. Energy Fuels 2010;24(7):3898–905.
[23] Sandford M, Page G, Crawford P. The all new AJV8. SAE 2009-01-1060; 2009.
[24] Bai Y, Wang Z, Wang J. Knocking suppression using stratified stoichiometric mixture in a DISI engine. SAE 2010-01-0597; 2010.
[25] Wang T, Peng Z, Liu SL, Xiao HD, Zhao H. Optimization of stratification combustion in a spark ignition engine by double-pulse port fuel injection. IMechE 2007;221:13.
[26] Heywood JB. Internal combustion engine fundamentals. McGraw-Hill; 1988.
[27] Christensen M, Johansson B. Supercharged homogeneous charge compression ignition (HCCI) with exhaust gas recirculation and pilot fuel. SAE 2000-01-1835; 2000.
[28] Wyszynski LP, Stone RC, Kalghatgi GT. The volumetric efficiency of direct and port injection gasoline engines with different fuels. SAE 2002-01-0839; 2002.
[29] Engler-Pinto CM, Nadai LD. Volumetric efficiency and air–fuel ratio analysis for flex fuel engines. SAE 2008-36-0223; 2008.
[30] Stone R. Introduction to internal combustion engines, 3rd ed. Basingstoke: Macmillan Press Ltd.; 1999.
[31] Aleiferis PG, Malcolm JS, Todd AR, Cairns A, Hoffmann H. An optical study of spray development and combustion of ethanol, iso-octane and gasoline blends in a DISI engine. SAE 2008-01-0073; 2008.
[32] Cairns A, Stansfield P, Fraser N, Blaxill H. A study of gasoline–alcohol blended fuels in an advanced turbocharged DISI engine. SAE 2009-01-0138; 2009.
[33] Yeliana, Cooney C, Worm J, Naber JD. The calculation of mass fraction burn of ethanol–gasoline blended fuels using single and two-zone models. SAE 2008-01-0320; 2008.
[34] Harrington JA, Shishu RC. A single-cylinder engine study of the effects of fuel type, fuel stoichiometry, and hydrogen-to-carbon ratio and CO, NO, and HC exhaust emissions. SAE 730476; 1973.
[35] Cheng WK, Summers T, Collings N. The fast-response flame ionization detector. Prog Energy Combus Sci 1998;24(2):89–124.
[36] Wallner T, Miers SA. Combustion behavior of gasoline and gasoline/ethanol blends in a modern direct-injection 4-cylinder engine. SAE 2008-01-0077; 2008.
[37] Rönkkö T, Virtanen A, Kannosto J, Keskinen J, Lappi M, Pirjola L. Nucleation mode particles with a nonvolatile core in the exhaust of a heavy duty diesel vehicle. Environ Sci Technol 2007;41:6384–9.
[38] Tian G, Li H, Xu H, Li Y, Satish MR. spray characteristics study of DMF using phase doppler particle analyzer. SAE 2010-01-1505; 2010.
[39] Takatori Y, Mandokoro Y, Akihama K, Nakakita K, Tsukasaki Y, Iguchi S, et al. Effect of hydrocarbon molecular structure on diesel exhaust emissions part 2: effect of branched and ring structures of paraffins on benzene and soot formation. SAE 982495; 1998.
[40] Tosaka S, Fujiwara Y, Murayama T. The effect of fuel properties on particulate formation (the effect of molecular structure and carbon number). SAE 891881; 1989.